JOURNAL OF BIOMEDICAL OPTICS 4(4), 450–458 (OCTOBER 1999)

COMPARISON OF OPTICAL COHERENCE TOMOGRAPHY IMAGING OF CATARACTS WITH HISTOPATHOLOGY

Cheryl D. DiCarlo,[†] W. P. Roach,[‡] Donald A. Gagliano,[*] Stephen A. Boppart,[**] Daniel X. Hammer,[§] Ann B. Cox,[♯] and James G. Fujimoto[**]

[†]Uniformed Services University of the Health Sciences, Department of Anatomy and Cell Biology, Bethesda, Maryland; [‡]Uniformed Services University of the Health Sciences, Department of Preventive Medicine and Biometrics, Bethesda, Maryland; [*]United States Army War College, Carlisle, Pennsylvania; [**]Department of Electrical Engineering and Computer Science, Research Laboratory of Electronics Massachusetts Institute of Technology, Cambridge, Massachusetts; [§]Department of Biomedical Engineering, University of Texas, Austin, Texas; [♯]Radiofrequency Radiation Division, Armstrong Laboratory, Brooks AFB, Texas

(Paper JBO-225 received Nov. 30, 1998; revised manuscript received June 7, 1999; accepted for publication June 10, 1999.)

ABSTRACT

This paper presents a comparison of *in vivo* optical coherence tomography (OCT) captured cataract images to subsequent histopathological examination of the lenticular opacities. OCT imaging was performed on anesthetized Rhesus monkeys, known as the delayed effects colony (DEC), with documented cataracts. These monkeys were exposed to several types of radiation during the mid and late 1960s. The radiation and age related cataracts in these animals were closely monitored using a unique grading system developed specifically for the DEC. In addition to this system, a modified version of a common cataract grading scheme for use in humans was applied. Of the original 18 monkeys imaged, lenses were collected at necropsy from seven of these animals, processed, and compared to OCT images. Results showed a direct correlation between the vertical OCT images and the cataractous lesions seen on corresponding histopathologic sections of the lenses. Based on the images obtained and their corresponding documented comparison to histopathology, OCT showed tremendous potential to aid identification and characterization of cataracts. There can be artifactual problems with the images related to movement and shadows produced by opacities. However, with the advent of increased speed in imaging and multiplanar imaging, these disadvantages may easily be overcome.
 [S1083-3668(99)00404-9]

Keywords cataracts; histopathology; lens; monkey; optical coherence tomography.

1 INTRODUCTION

The primary clinical means for grading cataract formation is by clinical slit-lamp examination. A relatively new noninvasive technique called optical coherence tomography (OCT)[1–7] can be used to image the anterior segment and provide the examiner with an additional assessment of the lens. OCT has been described extensively elsewhere and is analogous to ultrasound B scan imaging except for OCT's use of light rather than acoustic waves. In OCT, two dimensional cross-sectional images of tissue microstructure are constructed by assembling adjacent optical ranging scans of backscatter light versus depth.

In this study, we present the first comprehensive *in vivo* OCT imaging of ocular lens opacities and compare them to histopathology from a colony of geriatric rhesus monkeys with age-related and radiation-induced cataracts. A preliminary study has been reported elsewhere.[8] The geriatric rhesus monkeys used in this study were from the Brooks Air Force Base Delayed Effects Colony (DEC).[9] During the 1960s, NASA and the USAF conducted joint research investigating the effects of ionizing radiation for the manned space program in rhesus monkeys. The survivors of the acute radiation effects were placed in the DEC. Now ranging in age from 35 to 40 yr old they represent some of the oldest rhesus monkeys in captivity. Coupled with the presentation of late onset of lenticular opacities, this group of nonhuman primates has laid the foundation for our scientific understanding of radiation-induced cataracts. Late cataract development was noted to occur in these monkeys more than 20 yr after radiation exposure.

Address correspondence to Cheryl D. DiCarlo. Tel: 301-295-1559; Fax: 301-295-1715; E-mail: dicarlo@mxb.usuhs.mil

1083-3668/99/$10.00 © 1999 SPIE

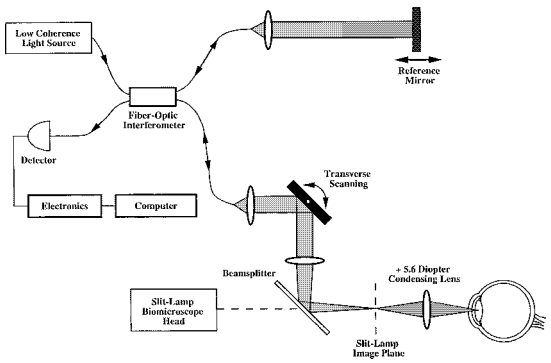

Fig. 1 Optical coherence tomography apparatus for imaging lenses (Ref. 8).

Age-related cataracts and radiation-induced cataracts have been evaluated in the control and exposed subjects semiannually by subjective ophthalmic slit-lamp examination for more than 10 yr. This colony provided an opportunity to image lenticular opacities of varying degrees of severity using slit-lamp, OCT, and histopathology. It is worth pointing out that this was the *first* and *only* time that *any* imaging technique, other than simple slit-lamp examination, was used to characterize the lenses of subjects from the DEC. Due to the unique nature of this monkey colony, collection of the lenses for histopathological exam was performed at the time of the natural demise of the animal in accordance with the established long-term protocol (generally by active euthanasia based on ''quality of life'' issues). At the time of necropsy, as outlined in the protocol, the prescribed method for lenticular tissue embedding in paraffin was utilized. Therefore, since original OCT images presented here were obtained in 1994, no extensive histopathologic comparison could be made for some years. No animal was euthanized specifically for this study. One animal was euthanized immediately after imaging, this decision was based strictly on the animal's failing geriatric condition and not on the use in this study. Animals involved in this study were procured, maintained, and used in accordance with the Federal Animal Welfare Act[10] and its amendments, the Guide for the Care and Use of Laboratory Animals[11] and Department of Defense Directive 3216.1.[12]

2 METHODS

All subjects were imaged using the OCT apparatus illustrated in Figure 1. The time-of-flight delay of light backscattered from lens structure is measured by low-coherence interferometry using a fiber optically integrated Michelson interferometer. Two dimensional tomographs of optical reflectivity are obtained by transverse scanning of the optical beam while performing sequential ranging measurements. Using an 843 nanometer superluminescent diode for the low coherent light source, resolutions of 45 μm in the transverse and 15 μm in the longitudinal direction are achieved. The longitudinal resolution is governed by the coherence length of the diode output and the transverse resolution by the spot size within the lens. A low numerical aperture (NA=0.012) was used to provide a large depth of field and a longer working distance. The instrument is integrated with a slit-lamp biomicroscope for *in vivo* exam of the lens and allows for the exact location within the lens to be determined while tomographical imaging is in process. A high resolution lens image consisting of the average of three scans was acquired in 60 s, while each scan used for averaging was obtained in 20 s. The logarithm of the image data is assigned a false-color scale and converted to a qualitative grading system for presentation. The color scale represents various degrees of optical backscatter from the tissue. The black to blue region represents no to low backscatter, the green to yellow represents a medium amount of backscatter, and orange to red indicates a high amount of backscatter.

Post-OCT imaging, all subjects were examined for clinical cataract grading using a Nikon biomicroscope slit-lamp (model No. 52819). Each lens examined in this manner was also photographed *in situ* using a 35 mm Nikon FM2 camera. The resolution of the slit-lamp photograph is approximately 5 μm. A comparison of the slit-lamp photographs to the OCT images is reported elsewhere.[8] The documented cataract grading of this colony was accomplished using the subjective grading system developed for radiation-induced cataracts[13] and a modified version of a common human cataract grading system.

Eighteen geriatric (ages 28–34 yr old) monkeys were maintained under standard laboratory conditions (12 h light/12 h dark). All of these animals used in this study were cared for and maintained in accordance with the ARVO statement for the use of animals in ophthalmic and vision research along with all federal and Department of Defense regulations. The 18 rhesus monkeys from the DEC (13 exposed and five control) were imaged using OCT and subsequently evaluated by slit-lamp examination. These monkeys were chemically restrained using 5–10 mg/kg ketamine HCl intramuscularly. Once restrained, two drops of 0.5% proparacaine HCl, 2.5% phenylephrine, and 1% tropicamide were administered to both eyes. The monkeys were then anesthetized using 10 mg/kg ketamine HCl and 0.25–0.50 mg/kg diazepam by intramuscular injection. Each imaged eye was stabilized by peribulbar injection of a sterile mixture of 2% lidocaine and hyaluronidase administered in 0.5–0.75 ml increments. Peribulbar injections were made in the superior nasal and inferior temporal aspects of the orbit. The monkeys were placed in a prone position on a three dimensional adjustable stage. A wire eye speculum was placed in the eye during OCT imaging. The eyes were kept moist us-

Table 1 Grading system for radiation-induced cataracts.[a]

Cataract grade	Lenticular characteristics
0	Suture lines visible only under direct illumination; lens clear; fundic details easily observed.
1	Prominent posterior or anterior suture lines; a few mild posterior cortical streaks or vacuoles may be observed; fundic details clear.
2	Prominent posterior or anterior sutures; anterior and/or posterior cortical streaks and vacuoles; fundus still observable.
3	Numerous anterior and posterior cortical streaks and/or vacuoles which may obscure suture opacities; nucleus relatively clear; fundus partially obscured.
4	Many anterior and posterior cortical opacities; fundic details not observable; fundic reflex still present.
5	Opaque lens; no fundic reflex.

[a] See Ref. 14.

ing 0.9% sterile saline. Immediately after imaging, the monkeys were examined using a slit lamp and the anterior segment of the eye was photographed using the slit-lamp camera. The monkeys' blood pressure and pulse were continuously monitored throughout the experimental protocol using a commercial blood pressure monitor, and pulse oximeter. The animals' body temperature was maintained with warm water blankets. One monkey (subject 1) was immediately euthanized as per approved protocol and the imaged eye was removed and fixed in Bouin's solution for routine light microscopy. All other animals in which samples were collected, six additional animals, were euthanized at various times, as described in Sec. 3, as per approved protocol.

The grading systems used in this study are listed in Ref. 9. The radiation induced grading system is based on the scale in Table 1. To more fully correlate with OCT findings, a modified version of the Lens Opacities Classification System III (LOCS III)[14] was used following imaging at the time of slit-lamp photography. The general rules of the LOCS III exclude the use of 0 when grading the lens and there are ten equal intervals between the grades. The grader decides if the image falls between reference standards and assesses a decimal grade. For example, if the image falls midway between grades 1 and 2, the grader would assess a grade of 1.5. For our purposes, using a modified version of LOCS III, if an image fell between two grades a + was used in place of a decimal. The LOCS III system grades nuclear color (NC) and nuclear opalescence (NO) on a scale of 1–6. NC grading is based on the cross-sectional view of the nucleus and the posterior subcapsular reflex. The color is then compared to the NC standards. The comparison of the average opalescence of the entire nucleus to the NO standard is the basis for the NO grade. The cortical and posterior subcapsular opacities under LOCS III are graded on a scale of 1–5. The cortical grade (*C*) is based on the standards compared to the retroillumination image focused either anteriorly at the plane of the iris or posteriorly at the posterior capsule. Our posterior subcapsular (PSC) grade is based on comparison of LOCS III standard *P* to the retroillumination image focused at the posterior of the lens. In addition, our modification to the LOCS III system included a grade for anterior subcapsular (ASC) opacities using a comparison of the standards for *P* to the retroillumination image focused anteriorly.

Following humane euthanasia, the monkeys' eyes were removed and fixed in either Bouin's or Formalin. After fixation and gross vertical sectioning, the samples were routinely prepared for paraffin embedding. Hematoxylin and eosin (H&E) stains were used for the histopathology presented in Sec. 3.

3 Results

Results from this study include acquisition of OCT images of the lenses in which the opacities were easily visualized in a vertical, horizontal, circular nuclear, and circular cortical plane. A comparison of the vertical OCT images to the vertically sectioned lens prepared for histopathology can be seen in Figures 2–8. This view was chosen for the ease of comparison to the slit-lamp images obtained. Of the original 18 geriatric rhesus monkeys imaged, only seven monkeys for a total of eight lenses will be discussed. This number is based on the ocular tissues available for comparison from this valuable colony at the time of this writing.

3.1 SUBJECT 1

The right eye of a 29 yr old rhesus with age-related cortical cataract grade of 2 is seen in Figure 2. The slit-lamp photo in Figure 2(a) shows a LOCS III grade of NO=2, NC=2, *C*=2, and ASC=1. The PSC grade of 3 was seen on exam and is not clearly shown in the slit-lamp photo. The vertical OCT image in Figure 2(b) when compared to the slit-lamp photo in Figure 2(a) shows the nuclear region in the medium reflectivity (green color) scale, the cortical region in the low to medium reflectivity (blue–green color) scale, the ASC area in the medium reflectivity (green color) scale, and the PSC area in the medium reflectivity (green to yellow) scale. The OCT image also confirms a visual (slit-lamp exam) identification of an irregular (wavy) anterior capsule. This anterior capsule irregularity was not clearly visualized on the slit-lamp photographs but is highly suspect on the photomicrograph of the lens seen in Figure 2(c). Also seen in Figure 2(c) are

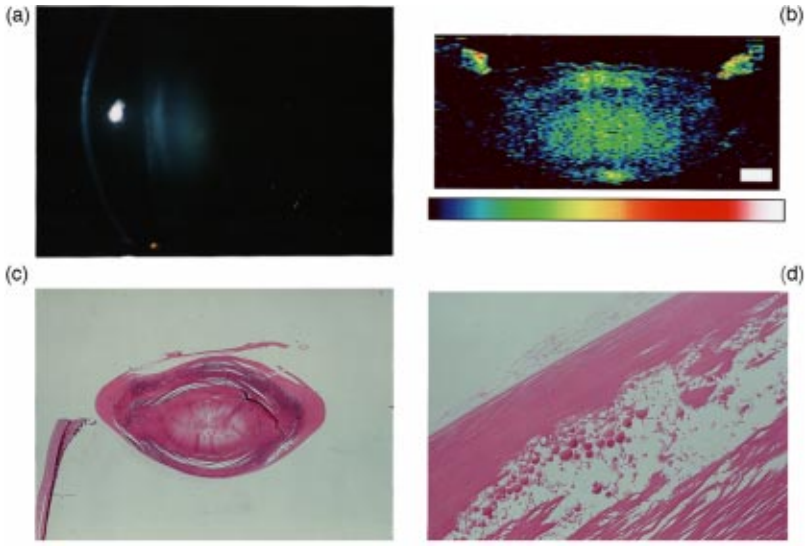

Fig. 2 Animal subject No. 1: (a) slit-lamp photo at 25× magnification (Ref. 8), (b) vertical OCT image with log reflection scale and white box equal to 1 mm in length (Ref. 8), (c) photomicrograph at 2.5× magnification (Ref. 8), and (d) photomicrograph at 40× magnification (Ref. 8).

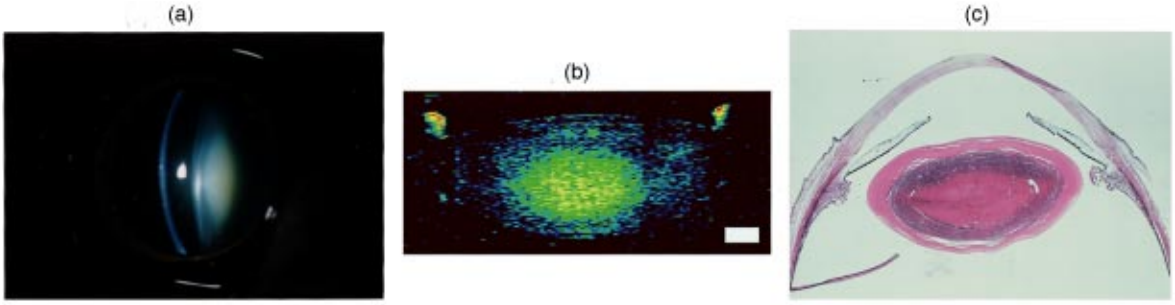

Fig. 3 Animal subject No. 2: (a) slit-lamp photo at 16× magnification, (b) vertical OCT image, (c) photomicrograph at 2.5× magnification.

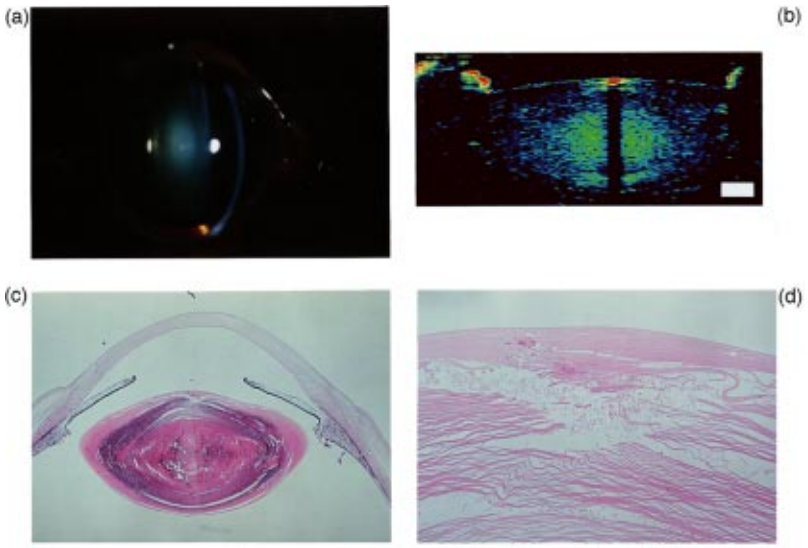

Fig. 4 Animal subject No. 3: (a) slit-lamp photo at 16× magnification, (b) vertical OCT image, (c) photomicrograph at 2.5× magnification, and (d) photomicrograph at 25× magnification.

the presence of cataracts at the PSC and ASC locations. The nucleus shows fixation artifact and there are separations in the lens tissue due to tissue sectioning artifact. On higher power views of the histopathology section, the lens has swollen lens fibers at the equators. Morgagnian globules are seen in the temporal aspect of the posterior subcapsular region [Figure 2(d) at 40× magnification]. The anterior capsule which is torn on the photomicrograph has an irregularity that without confirmation from OCT may have been disregarded during the slit-lamp examination.

3.2 SUBJECT 2

The right eye of a 32 yr old rhesus with age-related cortical cataract grade of 1 is seen in Figure 3. The slit-lamp photo [Figure 3(a)] confirms a LOCS III grade of NO=4, NC=3, *C*=1, ASC=1, and PSC =2. The OCT image [Figure 3(b)] shows a low to medium reflectivity (blue–green) in the ASC and PSC areas. The cortical area has medium reflectivity (green) and the nuclear area also has medium reflectivity that is slightly increased (green to yellow in color). A necropsy was performed on this animal 9 months after imaging. The photomicrograph [Figure 3(c)] shows a denser nucleus than cortical region thus separation of these regions are distinct. The ASC and PSC areas show some tissue separations probably due to the grades 1 and 2 cataracts, respectively, seen on examination.

3.3 SUBJECT 3

The left eye of a 30 yr old rhesus with radiation-induced/age-related cortical cataract grade of 2 is seen in Figure 4. The slit-lamp photo [Figure 4(a)] confirms a LOCS III grade of NO=1, NC=0, *C*=1, and ASC=1. The PSC grade was not assessed and also could not be seen well on the slit-lamp photograph. The OCT image [Figure 4(b)] shows high reflectivity (orange colored) in the ASC region, which shadows the tissues below preventing imaging of the central region. A necropsy was performed on this animal 9 months after imaging. The photomicrograph [Figure 4(c)] confirms a dense opacity in the ASC region that causes tissue fragmentation during sectioning. At higher magnification (25×) in Figure 4(d), the dense material is seen as an eosin intense area of the ASC region.

3.4 SUBJECT 4

The right eye of a 34 yr old rhesus with radiation-induced/age-related cortical cataract grade of 2 is seen in Figure 5. The slit-lamp photo [Figure 5(a)] confirms a LOCS III grade of NO=2, NC=1, *C*=1, ASC=2, and PSC=0. The vertical OCT image [Figure 5(b)] shows a medium to highly reflective (yellow to orange) area in the ASC region that shadows the tissue below. The nucleus is predominately of medium reflectance (green color) and the cortex is of low to medium reflectance (blue to green color). A necropsy was performed on this animal 12 months after imaging. The photomicrograph [Figure 5(c)] is from a cut that is slightly off center for a true vertical section but still represents the ASC area. A fracturing of the fibers during sectioning occurred, indicating a difference in tissue density between the ASC area and the cortex. On higher magnification (25×), Figures 5(d) and 5(e) show swollen fibers in the ASC area confirming the OCT and LOCS III grading.

3.5 SUBJECT 5

The right and left eyes of a 32 yr old rhesus with radiation-induced/age-related cortical cataract grade of 3 for each eye are seen in Figure 6. The slit-lamp photo for the right eye [Figure 6(a)] confirms a LOCS III grade of NO=4, NC=4, *C*=3+, ASC=2 but does not clearly show the PSC=3. The vertical OCT image [Figure 6(b)] shows ASC, PSC, and polar areas of medium reflectance (green colored). The cortex also has medium reflectance of slightly more intensity (green to yellow) and the nucleus has medium to high reflectivity (yellow to orange). A necropsy was performed on this animal 24 months after imaging. The photomicrograph [Figure 6(c)] shows only a partial section but clearly indicates a dense nucleus, cataractous fibers in the cortical region, and an ASC cataract. There are swollen fibers seen on higher magnification (25×) of the ASC [Figure 6(d)].

The slit-lamp photo for the left eye [Figure 6(e)] confirms a LOCS III grade of NO=4, NC=4, *C* =3+, ASC=2, and PSC=4. The OCT image [Figure 6(f)] shows a slightly irregular image of the anterior capsular area which was initially thought to be solely due to eye movement. This wavy appearance to the anterior capsule is seen on the histopathology section [Figure 6(g)]. The OCT image [Figure 6(f)] also shows the ASC, the PSC, and the nuclear areas have intense medium reflectance (predominately yellow colored) with the cortical area having low to medium reflectivity (blue to green colored). Unfortunately much of the nucleus is shattered from the paraffin sections [Figures 6(g)–6(i)] which is not an uncommon problem as differences in tissue density exist. The photomicrograph does nicely demonstrate the ASC and PSC cataracts. Higher magnification (25×) of the ASC and PSC areas show the fiber swelling and disorganization [Figures 6(h) and 6(i)] seen with cataracts.

3.6 SUBJECT 6

The right eye of a 28 yr old rhesus with age-related cortical cataract grade of 0+ is seen in Figure 7. The slit-lamp photo [Figure 7(a)] confirms a LOCS III grade of NO=1, NC=0, *C*=1, ASC=2, and PSC =0. The OCT image [Figure 7(b)] shows a slightly different grade for the PSC region which has medium to high reflectivity (yellow to orange) indicating a higher grade of cataract development much

closer to the grade assessed for the ASC region. A necropsy was performed on this animal 28 months after imaging. The entire lens was not captured on the slide from the paraffin section so only higher magnifications of lens fragments are shown. Figure 7(c) shows the photomicrograph section for the ASC area at 50× magnification. There are swollen fibers seen in the ASC region that are similar in amount to the swollen fibers seen in the PSC region in Figure 7(d) thus confirming the higher grade of cataract acquired earlier by the OCT image.

3.7 SUBJECT 7

The left eye of a 28 yr old rhesus with age-related cortical cataract grade of 1 is seen in Figure 8. The slit-lamp photo [Figure 8(a)] shows a LOCS III grade of NO=3, NC=2, C=3, ASC=1, and PSC =1. The vertical OCT image [Figure 8(b)] has medium reflectivity (green to yellow) for the ASC and PSC areas. The cortical area has low to medium reflectivity (blue to green) and the nuclear area has medium to high reflectivity (yellow to orange). A necropsy was performed on this animal 29 months after imaging. The photomicrograph [Figure 8(c)] shows a difference in the density between areas with the nuclear area being more dense. The separation between regions is also seen with the cortex and the subcapsular regions confirming the cataract formations seen in the ASC and PSC areas on OCT image.

4 DISCUSSIONS

The slit-lamp photographs obtained in this study are not as good as those that can be obtained in clinical ophthalmology for human medicine. Keeping in mind that the overall study was a laboratory animal research project using geriatric rhesus monkeys, the slit lamp was only used for the qualitative grading of opacities using the LOCS III system as a comparison to the radiation grading system developed and used by veterinary ophthalmologists for the DEC. Retroillumination images were obtained on some of the 18 animals studied but not for all. Further, a qualitatively description of lenticular opacity position and grade was made without its aid in all cases. In most clinical cases, this is the standard way in which cataract grading occurs, without the use of photos.

Shadowing was noted on some OCT images, namely, for subjects 3 and 4. Shadowing can be removed from the image by imaging slightly off the optical axis from the opacity causing the shadow. Motion artifacts such as eye movements and breathing artifacts, are easily identified because they extend throughout the lens and are not associated with an anterior density. Eye movement artifacts were seen in the left eye of subject 5 predominately on the nuclear circular and horizontal scans, which are not described here. Figure 6(f), the vertical scan of the left eye of subject 5, yielded minimal motion artifact which did not impair the ability to confirm the slit-lamp findings.

A small amount of movement can be averaged out of the image but correction for gross movement requires considerably more image processing, therefore peribulbar anesthesia along with good sedation or general anesthesia is currently required for this imaging in the DEC subjects. Although movement and shadow artifact can occur, these are readily identifiable and can be differentiated from underlying lenticular abnormalities. With the advent of increased speed in imaging and multiangle imaging, these disadvantages may easily be overcome. Histopathology verifies that OCT has tremendous potential to aid in identifying and characterizing lenticular opacities.

The prolonged time needed to obtain an image, dwell times of 20 s per image scan, will be very difficult at best for human patients. However for research and veterinary ophthalmology this is a very realistic time regime. In the 4 yr since the *in vivo* lenticular OCT images were obtained, the research grade OCT has been enhanced at Massachusetts Institute of Technology (MIT) for both image quality and dwell time down to a few seconds per scan. It is highly recommended that further research on OCT's ability to become a diagnostic tool for lenticular cataract be continued. Also, those studies should include Scheimphlug slit images for comparison with OCT as well as histology.

5 CONCLUSIONS

Of the 18 geriatric rhesus imaged to date, seven have had tissues collected and processed for comparison via OCT images and light microscopy. OCT confirmed all lenticular opacities described via the slit-lamp biomicroscope with additional opacities identified that had been missed on simple slit-lamp examination. OCT identified two irregular anterior capsules within this group. One was suspect on slit-lamp exam, while the other was originally thought to be movement on the OCT image. Subsequent histopathology confirmed that both of these were irregular capsules (subjects 1 and 5).

OCT was able to view lens opacities missed by simple slit-lamp examination as previously mentioned, and this should be of importance to clinicians or researchers grading opacities in long term studies. Scheimphlug cameras are highly praised by ophthalmologists and researchers for their ability to provide exquisite lenticular images. However, Scheimphlug is exceedingly costly and requires extensive training for operation. At the time of the OCT lenticular images obtained in this study only five were available in the United States and none were available in the state of Texas. OCT could offer an appropriate, cost effective alternative for lenticular imaging in the future. One hope is for further studies that will use the OCT gray-scale images

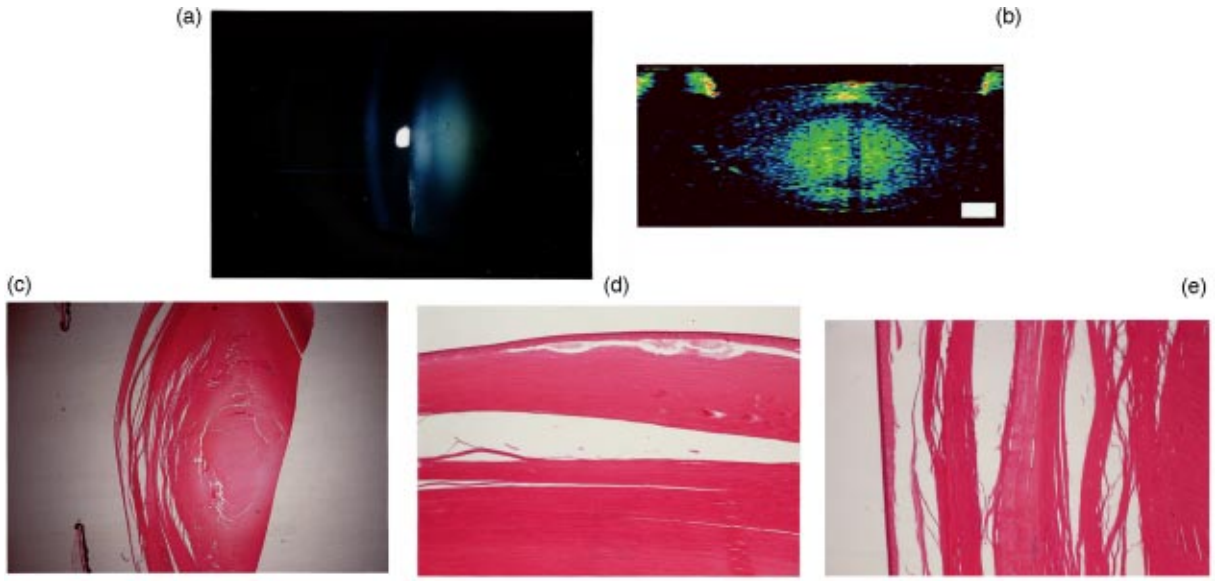

Fig. 5 Animal subject No. 4: (a) slit-lamp photo at 25× magnification, (b) vertical OCT image, (c) photomicrograph at 5.0× magnification, (d) photomicrograph at 25× magnification, and (e) photomicrograph at 25× magnification.

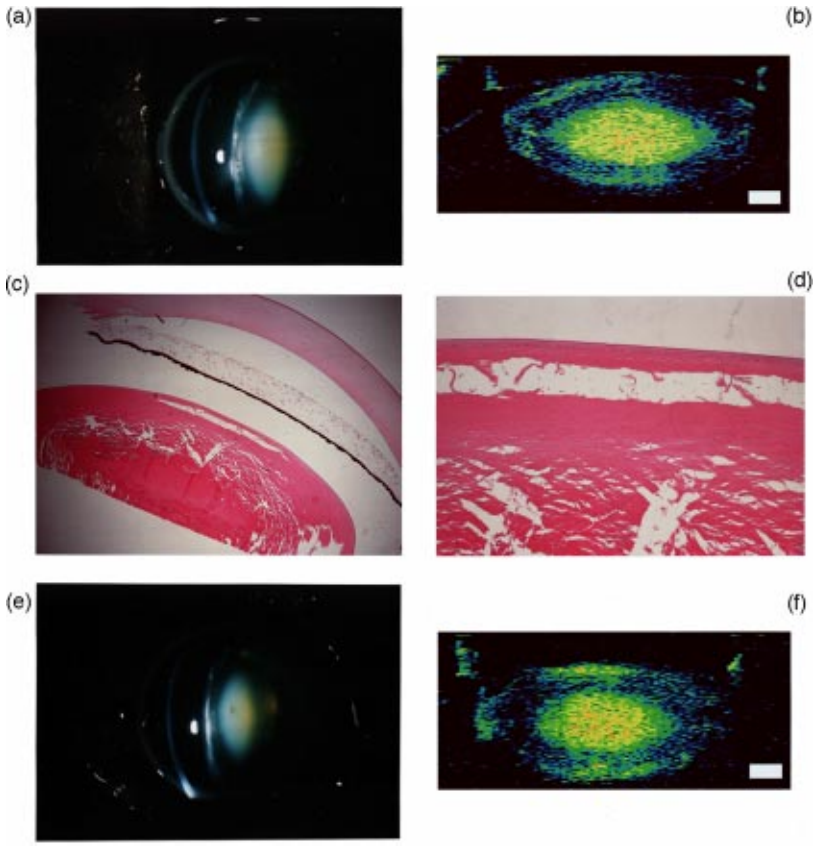

Fig. 6 Animal subject No. 5: (a) OD (right eye) slit-lamp photo at 25× magnification and (e) OS (left eye) slit-lamp photo at 16× magnification, (b) and (f) vertical OCT images, OD and OS, respectively, (c) photomicrograph at 5.0× magnification, (d) photomicrograph at 25× magnification, (g) photomicrograph at 5.0× magnification, (h) photomicrograph at 25× magnification, and (i) photomicrograph at 25× magnification.

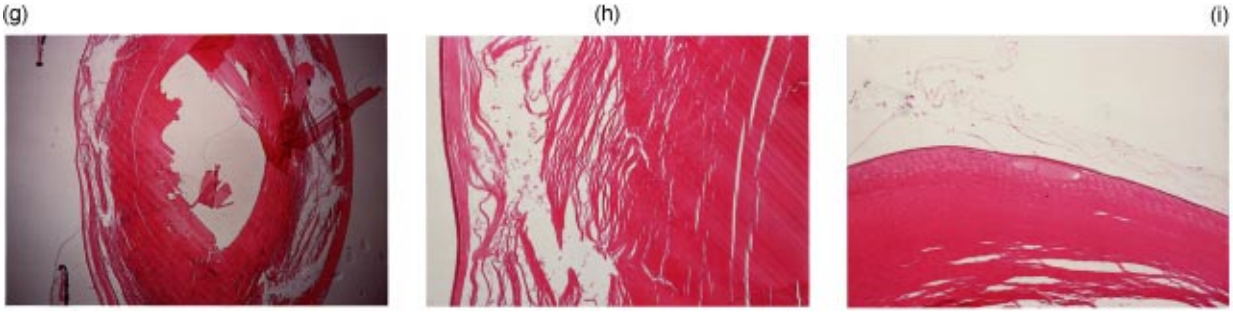

Fig. 6 (*Continued*).

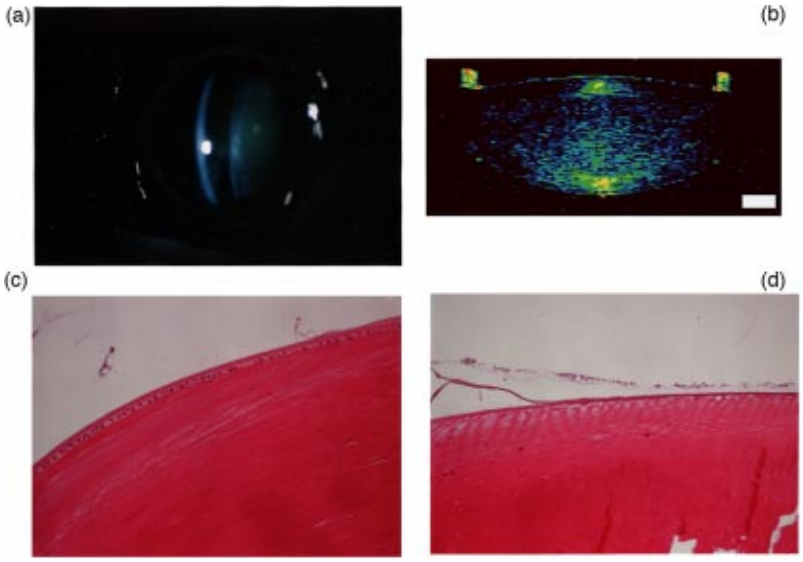

Fig. 7 Animal subject No. 6: (a) slit-lamp photo at 16× magnification, (b) vertical OCT image, (c) photomicrograph at 50× magnification, and (d) photomicrograph at 50× magnification.

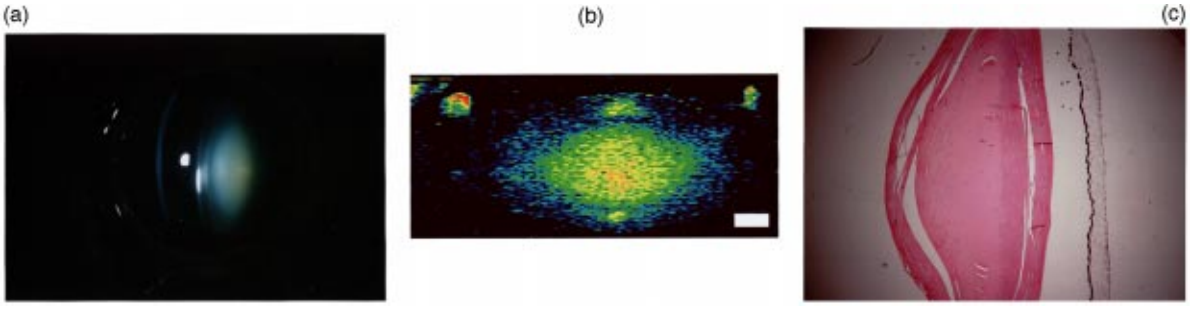

Fig. 8 Animal subject No. 7: (a) slit-lamp photo at 16× magnification, (b) vertical OCT image, (c) photomicrograph at 5.0× magnification.

for quantitatively assessing lenticular opacities, thereby eliminating the subjective nature of lenticular cataract diagnosis.

Acknowledgments

All of the experimental work was conducted at the Laser Laboratory, Optical Radiation Division (AL/OE), Armstrong Laboratory, Brooks Air Force Base under Air Force Office of Scientific Research Grant No. 2312A101, the Armstrong Laboratory Contract No. F33615-92-C-0017, and the National Aeronautics and Space Administration Contract No. T-13215. We wish to further acknowledge the efforts of Technical Sergeant Rodney Amnotte and Audrey B. Smith for their technical expertise in handling the animals during examination and imaging and Dr. Dale Payne for his computer assistance with photoimage processing. We would also like to acknowledge Dr. Michael Hee for his assistance in the optics setup of the OCT unit and Dr. Eric Swanson, MIT Lincoln Laboratory, for granting the use of the OCT unit. Additionally, we wish to thank Dr. Martha Hanes, University of Texas Health Sciences Center and Staff Sergeant Joe N. Golden, Veterinary Pathology Branch (AL/OEVP), Armstrong Laboratory for their direct support of the histopathology and Dr. Frank E. Cheney, Jr., and Dr. Ben Rockwell, Optical Radiation Division (AL/OEO), Armstrong Laboratory for their instruction and information on the use of the slit-lamp camera, along with Dr. A.C. Lee, Colorado State University, for the use of the previously collected radiation induced cataract data.

References

1. M. R. Hee et al., ''Optical coherence tomography of macular holes,'' *Ophthalmology* **102**, 748–756 (1995).
2. M. R. Hee et al., ''Optical coherence tomography of the human retina,'' *Arch. Ophthalmol. (Chicago)* **113**, 325–332 (1995).
3. M. R. Hee et al., ''Optical coherence tomography of central serous chorioretinopathy,'' *Am. J. Ophthalmol.* **120**, 65–74 (1995).
4. D. Huang et al., ''Optical coherence tomography,'' *Science* **254**, 1178–1181 (1991).
5. J. A. Izatt et al., ''Micron-resolution imaging of the anterior eye *in vivo* with optical coherence tomography,'' *Arch. Ophthalmol. (Chicago)* **112**, 1584–1589 (1994).
6. J. A. Izatt et al., ''Ophthalmic diagnostics using optical coherence tomography,'' in *Proceedings of Ophthalmic Technologies III*, *Proc. SPIE* **1877**, 136–144 (1993).
7. C. A. Puliafito et al., ''Imaging of macular diseases with optical coherence tomography,'' *Ophthalmology* **102**, 217–229 (1995).
8. C. D. DiCarlo et al., ''A new noninvasive imaging technique for cataract evaluation in the rhesus monkey,'' in *Lasers in Surgery: Advanced Characterization, Therapeutics, and Systems V*, *Proc. SPIE* **2395**, 636–643 (1995).
9. A. B. Cox et al., ''Progress in the Extrapolation of Radiation Cataractogenesis Data Across Longer-Lived Mammalian Species,'' *Biological Effects and Physics of Solar and Galactic Cosmic Radiation, Part A*, Plenum Press, New York (1993).
10. ''Code of Federal Regulations,'' Title 9, ''Animal Welfare Act,'' U.S. Government Printing Office (1996).
11. Institute of Laboratory Animal Resources Commission on Life Sciences National Research Council, *Guide for the Care and Use of Laboratory Animals*, National Academy Press, Washington, D.C. (1996).
12. Department of Defense Directive 3216.1, *Use of Animals in DoD Programs*, U.S. Government Printing Office, Washington, D.C. (1995).
13. L. T. Chylack, Jr. et al., ''The lens opacities classification system III,'' *Arch. Ophthalmol. (Chicago)* **111**, 831–836 (1993).
14. P. C. Keng, A. C. Lee, A. B. Cox, D. S. Bergtold, and J. T. Lett, ''Effects of heavy ions on rabbit tissues: cataractogenesis,'' *Int. J. Radiat. Biol.* **41**(2), 127–137 (1982).